# DENSIFICATION RATES OF SNOW AT POLAR GLACIERS*

Norikazu MAENO

*The Institute of Low Temperature Science, Hokkaido University,
Kita-19, Nishi-8, Kita-ku, Sapporo 060*

**Abstract:** The densification process of snow at polar glaciers is explained as a pressure sintering phenomenon, and the strain rates of snow densification obtained from density-depth relationships at two polar sites are discussed in terms of pressure sintering parameters. It is found that the power law and diffusional creep mechanisms are important at shallower and deeper depths respectively than the depth of air bubble close-off.

## 1. Introduction

Though the densification of dry snow and its transformation into ice have often been studied, most of the work has aimed at obtaining an empirical relationship between density and depth/time applicable to different polar sites. In the present study the densification process of snow is explained as a pressure sintering process of ice particle compacts; the present paper gives an estimate of strain rates of snow densification at two sites on the Antarctic Ice Sheet and an explanation of them in terms of pressure sintering parameters.

## 2. Characteristics of Snow Densification and Its Rates at Polar Glaciers

It is generally recognized that the snow densification process at polar glaciers can be divided into three stages by two critical densities (PERUTZ and SELIGMAN, 1939; BENSON, 1962; ANDERSON and BENSON, 1963; LANGWAY, 1967); snow deposits densify firstly by mechanical destruction and packing of snow particles till the first critical density, $550 \text{ kg} \cdot \text{m}^{-3}$, secondly by plastic deformation and recrystallization till the second critical density, $820–840 \text{ kg} \cdot \text{m}^{-3}$, and finally by the shrinkage of entrapped air bubbles until the theoretical density of ice ($917 \text{ kg} \cdot \text{m}^{-3}$) is reached. According to ANDERSON and BENSON (1963), the first critical density corresponds to the maximum packing density that can be attained with granular aggregates. The second critical density is explained as follows: at the density intercommunicating air channels in snow are pinched off and entrapped as air bubbles in ice.

The existence of an additional critical density, $730 \text{ kg} \cdot \text{m}^{-3}$, was suggested by MAENO (1978; MAENO *et al.*, 1978) on the basis of electrical measurements of

---

* Contribution No. 2432 from the Institute of Low Temperature Science, Hokkaido University.
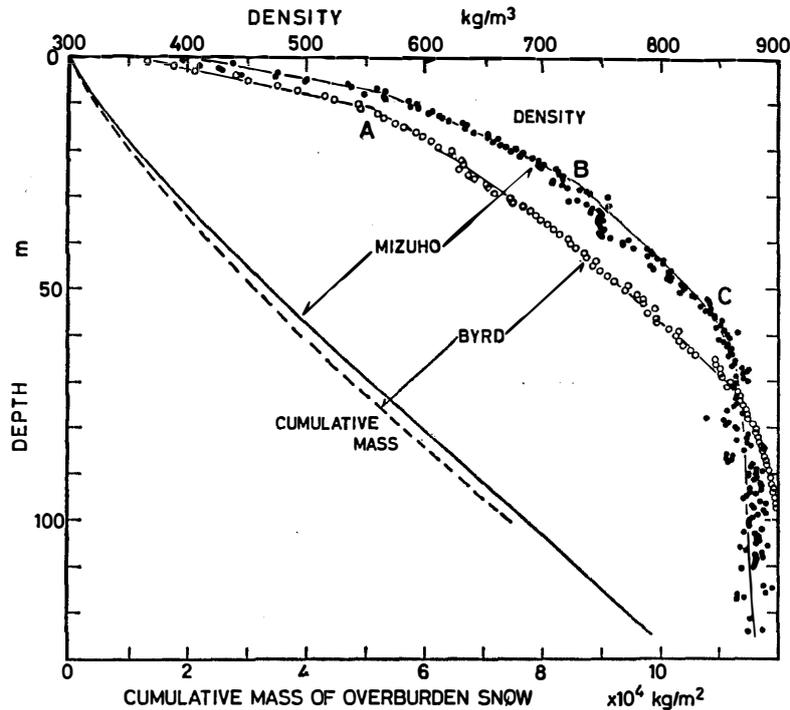
Fig. 1. Density and cumulative mass of overburden snow versus depth at Mizuho and Byrd Stations. Data are after NARITA and MAENO (1978) and GOW (1968).

Antarctic snow cores; At the density bonding and packing mode of constituent snow particles reaches an optimum state, that is, the contact between particles becomes a maximum and air bubbles are only included as thin cylinders along intersections of several grain boundaries.

Figure 1 shows two typical examples of density-depth profiles of snow obtained by measurements on core samples drilled at Mizuho Station (70°41'53"S, 44°19'54"E; 2230 m above sea level; ice thickness 2095 m; mean annual temperature −33°C) and Byrd Station (80°01'S, 119°32'W; 1500 m above sea level; ice thickness 2500 m; mean annual temperature −28°C) in Antarctica. In the figure the three critical densities are indicated as **A**, **B** and **C**, and the cumulative mass of overburden snow per unit area is also given. Numerical data used are given in NARITA and MAENO (1978) and Gow (1968).

The density-depth relationships were converted to density-cumulative mass relationships in Fig. 2, in which the slopes of curves directly give the densification rates. The densification process was divided into four stages (**I, II, III** and **IV**) according to the above discussion, and in each stage the density was assumed to be a linear function of cumulative mass. Exponential and logarithmic functions were also examined to fit the data, but no special merits were noted. Correlation coefficients in fitting linear functions were above 0.93 in every stage of the Mizuho and Byrd cores except stage **IV** of the Mizuho cores, in which the correlation coefficient was as small as 0.719. The unsatisfactory correlation seems to be due to the existence of tiny cracks contained in the core samples as will be discussed in more detail later.
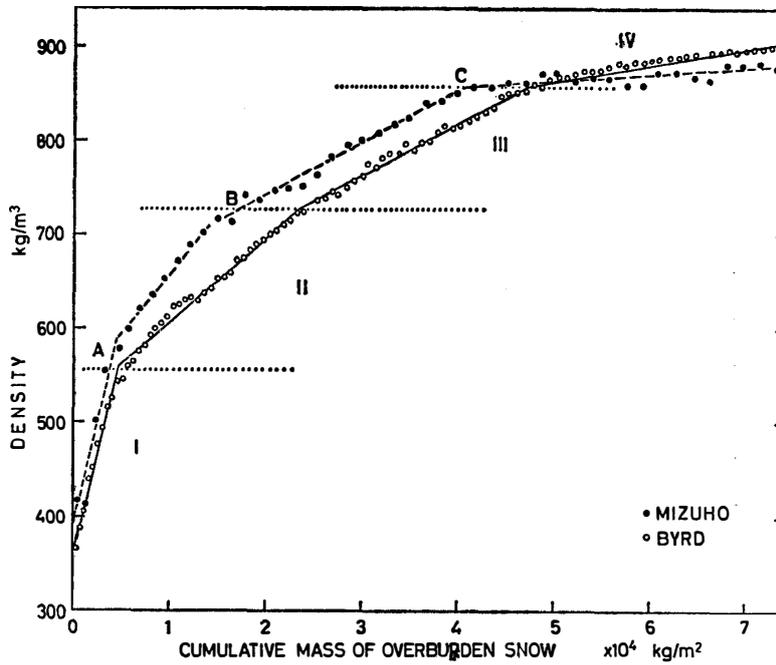
Fig. 2.   Density versus cumulative mass of overburden snow.  Four stages,
I, II, III and IV are indicated.

The strain rate of snow densification ($\dot{\varepsilon}$) is defined as

$$\dot{\varepsilon} = \dot{\rho}/\rho ,\tag{1}$$

where $\dot{\rho}$ is the densification rate of snow at density $\rho$. The cumulative mass of overburden snow per unit area ($\sigma$) at a certain depth is written as

$$\sigma = at ,\tag{2}$$

where $a$ is the accumulation rate of snow and $t$ is the time.  Then assuming a steady state the strain rate in each stage can be estimated from the slopes of straight lines in Fig. 2.  The steady-state assumption corresponds to that of so-
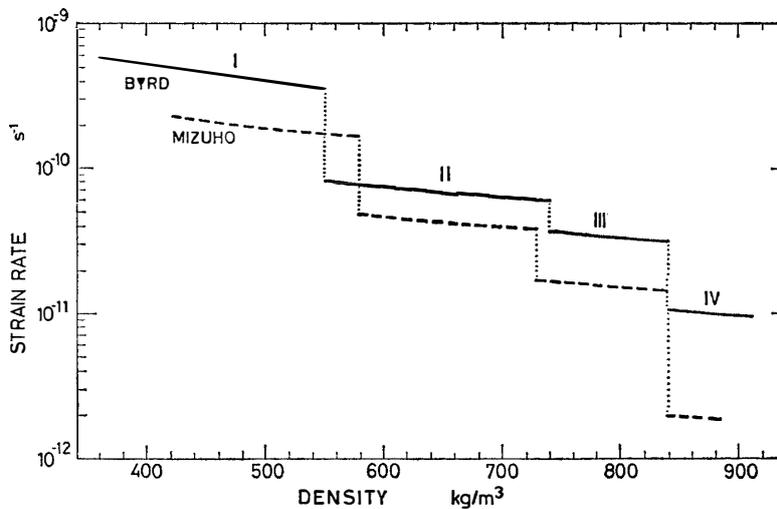


Fig. 3.   Strain rate of snow densification estimated from slopes of straight
lines in Fig. 2.

called Sorge's law of snow density profile (BADER, 1953).

The results are given in Fig. 3; in the estimate accumulation rates were taken to be

$$a = 70 \ \text{kg} \cdot \text{m}^{-2} \cdot \text{year}^{-1} = 2.22 \times 10^{-6} \ \text{kg} \cdot \text{m}^{-2} \ \text{s}^{-1}$$

at Mizuho Station (MAENO and NARITA, 1979) and

$$a = 157 \ \text{kg} \cdot \text{m}^{-2} \cdot \text{year}^{-1} = 4.98 \times 10^{-6} \ \text{kg} \cdot \text{m}^{-2} \ \text{s}^{-1}$$

at Byrd Station (Gow, 1968). It is noted that the strain rate of snow densification at the two sites ranges from $10^{-12}$ to $10^{-9} \ \text{s}^{-1}$ and its magnitude is almost constant within each stage in spite of the increase in the cumulative mass, that is the driving force for the snow densification. The discontinuous decrease in the strain rate suggests a change of the densification mechanism. The large strain rate for Byrd Station is considered to be due to the warmer temperature, larger accumulation rate and other climatic differences.

## 3. Discussion

In our previous paper (MAENO and NARITA, 1979) the strain rate of snow densification at Mizuho Station was assumed to be proportional to the applied compressive pressure due to the overburden snow; the snow was considered to be a Newtonian viscous material and a coefficient of proportionality, named the compactive viscosity coefficient, was estimated. However, these analyses are not satisfactory when the physical mechanisms involved are examined; in fact the results presented in the previous section have shown the existence of four stages of different strain rates, and therefore possibly different mechanisms. We discuss here the densification processes in stages **III** and **IV**, in which relative motions of individual ice particles are almost excluded and the predominant process of densification is plastic deformation.

Diffusion models for the densification of powder compacts have been presented by COBLE (1970): according to the models the strain rate of densification of a snow compact is written as

$$\dot{\varepsilon} = \dot{\rho}/\rho = \frac{40 D_l \Omega}{3 d^2 kT} \left( \frac{\rho_i \tau}{\rho} + \frac{\gamma}{r} \right) \tag{3}$$

for lattice diffusion, and

$$\dot{\varepsilon} = \frac{148 D_b \delta \Omega}{d^3 kT} \left( \frac{\rho_i \tau}{\rho} + \frac{\gamma}{r} \right) \tag{4}$$

for grain boundary diffusion. Here $d$ is the grain diameter, $k$ is the Boltzmann's constant, $r$ is the radius of pore, $T$ is the temperature, $\delta$ is the width of the grain boundary, $\gamma$ is the surface energy of ice, $\rho_i$ is the theoretical density of ice, $\Omega$ is the molecular volume of ice, and $\tau$ is the applied stress. $D_l$ and $D_b$ are respectively lattice and grain boundary diffusion coefficients, and are expressed as

$$D_l = D_{l0} \exp \left( - E_l / kT \right), \tag{5}$$

and

$$D_b = D_{b0} \exp \left( - E_b / kT \right), \tag{6}$$

where $D_{l0}$ and $D_{b0}$ are pre-exponential constants, and $E_l$ and $E_b$ are the activation

energies for lattice and grain boundary diffusions respectively.

Equations (3) and (4) are essentially the Nabbaro-Herring and Coble creep equations which are often applied to creep behavior of polycrystalline materials. A variation is the introduction of an effective stress in the porous mass, $\rho_i\,\tau/\rho$, insfead of $\tau$.

For the plastic deformation caused by the movement of dislocations, a power law creep model presented by WILKINSON and ASHBY (1975) is used:

$$\dot{\varepsilon} = \frac{2A(1-\rho/\rho_i)}{\{1-(1-\rho/\rho_i)^{1/n}\}^n}\left(\frac{2\tau}{n}\right)^n \qquad (7)$$

for cylindrical pores, and

$$\dot{\varepsilon} = \frac{3A(1-\rho/\rho_i)}{2\{1-(1-\rho/\rho_i)^{1/n}\}^n}\left[\frac{3}{2n}\left\{\tau-\frac{(\rho_i-\rho_0)\rho}{(\rho_i-\rho)\rho_0}\,p_0\right\}\right]^n \qquad (8)$$

for spherical pores containing air. Here $A$ and $n$ are constants appearing in the following empirical power law of creep:

$$\text{Strain rate} = A\tau^n = B\tau^n \exp\left(-E_c/kT\right), \qquad (9)$$

where $B$ is a constant and $E_c$ is the activation energy for the mechanical creep. $p_0$ is the initial internal air pressure within pores when the bulk density is $\rho_0$.

The strain rate of snow densification was estimated using eqs.(3)–(9) for

Table 1. Symbols and numerical values.

| | | | |
|---|---|---|---|
| Molecular volume | $\Omega$ | $3.27\times10^{-29}$ m$^3$ | |
| Boltzmann's constant | $k$ | $1.38\times10^{-23}$ J·K$^{-1}$ | |
| Pre-exponential for lattice diffusion constant | $D_{l0}$ | $3.0\times10^{-2}$ m$^2$·s$^{-1}$ | ITAGAKI (1964) |
| Pre-exponential for grain boundary diffusion constant | $D_{b0}$ | $D_{l0}$ | |
| Activation energy for lattice diffusion | $E_l$ | $66.2$ kJ·mol$^{-1}$ | ITAGAKI (1964) |
| Activation energy for grain boundary diffusion | $E_b$ | $(2/3)E_l$ | |
| Theoretical density of ice | $\rho_i$ | $917$ kg·m$^{-3}$ | |
| Surface energy of ice | $\gamma$ | $0.1$ J·m$^{-2}$ | |
| Width of grain boundary | $\delta$ | $2b$ | |
| Burgers vector of dislocation | $b$ | $4.5\times10^{-10}$ m | |
| Pre-exponential for dislocation creep | $B$ | $9.72\times10^7$ s$^{-1}$ (MN$^{-1}$m$^2$)$^n$ | BARNES et al. (1971) |
| Stress exponent | $n$ | $3.08$ | BARNES et al. (1971) |
| Activation energy for creep | $E_c$ | $74.5$ kJ·mol$^{-1}$ | |
| Accumulation rate of snow | $a$ | $70$ kg·m$^{-2}$ year$^{-1}$ (Mizuho Station) | MAENO and NARITA (1979) |
| | | $157$ kg·m$^{-2}$ year$^{-1}$ (Byrd Station) | Gow (1968) |
| Initial air pressure of pores | $p_0$ | $74.5$ kPa (Mizuho Station) | |
| | | $80.6$ kPa (Byrd Station) | |

Mizuho and Byrd Stations. Numerical values used are listed in Table 1. The initial air pressure of pores, $p_0$, was assumed to be the present mean air pressure and the close-off density, $\rho_0$, was taken to be $840\ \mathrm{kg\cdot m^{-3}}$. The diameters of ice particles, $d$, become larger with depth, therefore with time: the following empirical relationships were used,

$$d^2 = 1.02 \times 10^{-6} + 1.34 \times 10^{-16}t \quad \mathrm{m^2} \tag{10}$$

at Mizuho Station (after the data given by NARITA and MAENO, 1979), and

$$d^2 = 6.0 \times 10^{-7} + 3.81 \times 10^{-16}t \quad \mathrm{m^2} \tag{11}$$

at Byrd Station (GOW, 1971), where $t$ is the time (seconds) after deposit on the surface of the Ice Sheet. It is known that the growth rate of ice particles varies with depth at Mizuho Station, but eq.(10) obtained at depths shallower than 35 m, was used in the present calculation.

The surface energy terms in eqs.(3) and (4) were considered negligibly small in the present pressure sintering estimate: since the radii of air pores in Antarctic snow are roughly 100 $\mu$m (MAENO et al., 1978), the magnitude of $\gamma/r$ is of the order of 1 kPa, which can be neglected as compared with the applied stress, e.g. 200 kPa at the density of $700\ \mathrm{kg\cdot m^{-3}}$ (Mizuho Station).

Though the models used are too simple to describe the complex densification processes of snow, the results given in Figs. 4 and 5 show that the densification rates before and after the close-off of air channels can be roughly simulated with power law and diffusional creep equations respectively. It is possible to get values nearer to the measured ones with a small adjustment of parameters, which is not given here since it does not seem to bear an obvious physical meaning and the detailed processes involved are not yet understood.
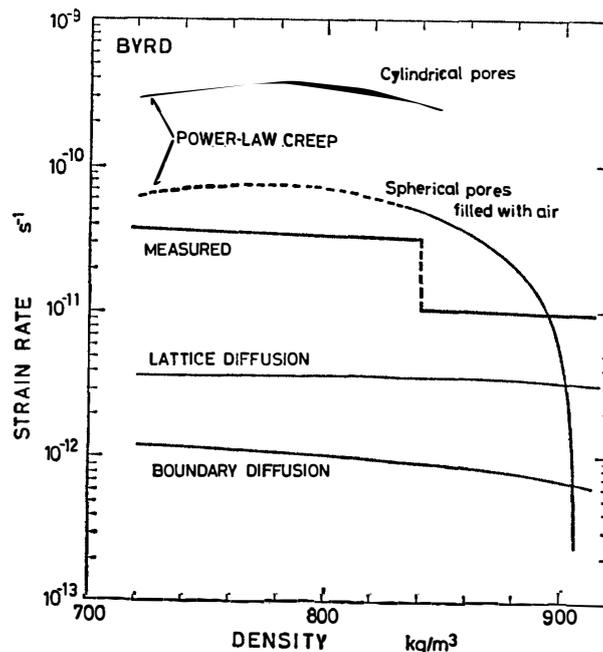


Fig. 4.  Strain rate of snow densification in stages III and VI at Byrd Station.
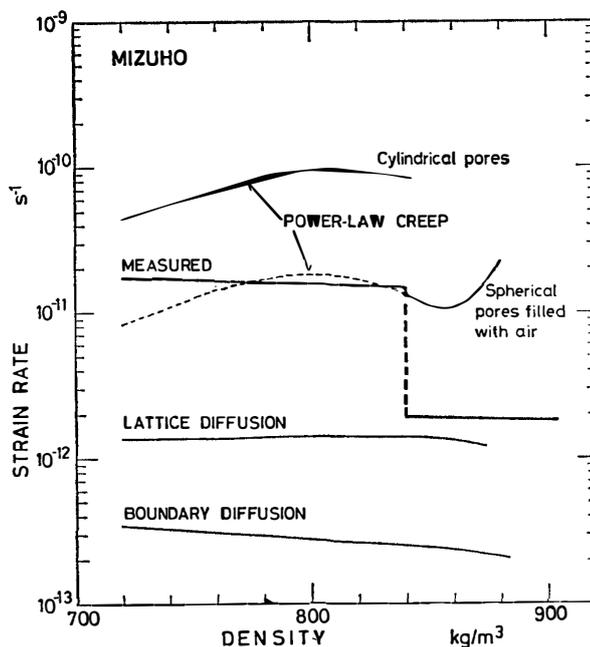
*Fig. 5. Strain rate of snow densification in stages III and IV at Mizuho Station.*

After the close-off of air bubbles, the internal air pressure increases as the densification proceeds, and the effective stress decreases. Consequently the contribution of power law creep reduces rapidly, and that of diffusional creep becomes more important. The tendency of increase in the calculated strain rate due to power law creep at Mizuho Station (Fig. 5) is considered to be caused by the errors involved in the measured densities: according to the observations by Narita *et al.* (1978) cores recovered below about 70 m depth (roughly 860 kg·m$^{-3}$) contained various mechanical disturbances such as tiny cracks.

## Acknowledgments

## References

Anderson, D. L. and Benson, C. S. (1963): The densification and diagenesis of snow. Ice and Snow, Properties, Processes and Applications, ed. by W. D. Kingery. Cambridge, The MIT Press, 391–411.

Bader, H. (1953): Sorge's law of densification of snow on high polar glaciers. SIPRE Res. Pap., **2**, 3 p.

Barnes, P., Tabor, D. and Walker, J. C. F. (1971): The friction and creep of polycrystalline ice. Proc. R. Soc. London, Ser. A, **324**, 127–155.

Benson, C. S. (1962): Stratigraphic studies in the snow and firn of the Greenland ice sheet. SIPRE Res. Rep., **70**, 139 p.

COBLE, R. L. (1970): Diffusion models for hot pressing with surface energy and pressure effects as driving forces. J. Appl. Phys., 41(12), 4798–4808.

GOW, A. J. (1968): Deep core studies of the accumulation and densification of snow at Byrd Station and Little America V, Antarctica. CRREL Res. Rep., 197, 45 p.

GOW, A. J. (1971): Depth-time-temperature relationships of ice crystal growth in polar glaciers. CRREL Res. Rep., 300, 18 p.

ITAGAKI, K. (1964): Self-diffusion in single crystals of ice. J. Phys. Soc. Japan, 19, 1081.

LANGWAY, C. C., Jr. (1967): Stratigraphic analysis of a deep core from Greenland. CRREL Res. Rep., 77, 130 p.

MAENO, N. (1978): The electrical behaviors of Antarctic ice drilled at Mizuho Station, East Antarctica. Mem. Natl Inst. Polar Res., Spec. Issue, 10, 77–94.

MAENO, N. and NARITA, H. (1979): Compactive viscosity of snow and its climatic implications at Mizuho Station, Antarctica. Nankyoku Shiryô (Antarct. Rec.), 67, 18–31.

MAENO, N., NARITA, H. and ARAOKA, K. (1978): Measurements of air permeability and elastic modulus of snow and firn drilled at Mizuho Station, East Antarctica. Mem. Natl Inst. Polar Res., Spec. Issue, 10, 62–76.

NARITA, H. and MAENO, N. (1978): Compiled density data from cores drilled at Mizuho Station. Mem. Natl Inst. Polar Res., Spec. Issue, 10, 136–158.

NARITA, H. and MAENO, N. (1979): Growth rates of crystal grains in snow at Mizuho Station, Antarctica. Nankyoku Shiryô (Antarct. Rec.), 67, 11–17.

NARITA, H., MAENO, N. and NAKAWO, M. (1978): Structural characteristics of firn and ice cores drilled at Mizuho Station, East Antarctica. Mem. Natl Inst. Polar Res., Spec. Issue, 10, 48–61.

PERUTZ, M. and SELIGMAN, G. (1939): A crystallographic investigation of glacier structure and mechanism of glacier flow. Proc. R. Soc. London, Ser. A, 172, 335–359.

WILKINSON, D. S. and ASHBY, M. F. (1975): Pressure sintering by power law creep. Acta Metall., 23(11), 1277–1285.